Composites Engineering, Vol. 3, Nos 7–8, pp. 661–674, 1993.
Printed in Great Britain.

0961-9526/93 $6.00 + .00

DETERMINATION OF TRANSIENT AND STEADY-STATE CREEP OF METAL-MATRIX COMPOSITES BY A SECANT-MODULI METHOD

H. H. PAN and G. J. WENG

Department of Mechanical and Aerospace Engineering, Rutgers University, New Brunswick, NJ 08903, U.S.A.

Abstract—A theoretical model which can reflect the weakening constraint power of the ductile matrix in the course of creep deformation is established to estimate the development of transient and steady-state creep strain of a fiber-reinforced metal-matrix composite. This method makes use of the secant moduli of the elastic-creeping matrix in the construction of a linear comparison composite, and, when coupled with an energy approach recently proposed by Qiu and Weng (1992, *J. appl. Mech.*, **59**, 261–268), it can also account for the effect of non-uniform stress fields on the overall creep to a certain extent. The theory is applied to a Borsic/aluminium system to examine the anisotropic creep behavior along the axial and transverse directions. As compared to the predictions of Zhu and Weng's (1990, *Mech. Mater.* **9**, 93–105) mean-field theory and Wang and Weng's (1992, *ASME J. Engng Mater. Tech.* **114**, 237–244) local theory (both were based on the elastic constraint and were intended for the small creep range), the results are close to both along the axial directions, but along the transverse direction the secant-moduli method is found to provide a softer response for the composite. A direct comparison to the experimental data under transverse tension shows that the theory is quite accurate even at 35% of fiber volume fraction. The theoretical model is finally employed to estimate the growth of the maximum interfacial tensile stress under a transverse loading with and without a superimposed lateral compression, and it is found that, such a local tension, which is responsible for the onset of interfacial cracking, can grow quite significantly during the creep process, especially with the assistance of the lateral compression.

1. INTRODUCTION

The high-temperature creep strength is known to be the most critical factor for the design of gas turbine blades in an aircraft engine. Traditionally, these blades are made of nickel-based superalloys, whereas in recent years both single crystals and polycrystals with directionally solidified columnar grains have also been used in the hot section of the engine. The idea to implement the latter class of materials is to remove the presence of grain boundaries perpendicular to the radial direction so that, under a centrifugal force, no creep cavitation along such boundaries would develop. The creep behavior of single crystals and columnar grains are both anisotropic, with the grain orientations deliberately grown so as to yield the highest possible strength along the loading direction.

Fiber-reinforced metal-matrix composites (MMC) represent another class of potential high-temperature materials. These composites provide both high strength and high ductility, and, when the fibers are aligned radially, their strengthening effect is similar to a polycrystal with columnar grains. Better still, the fabrication process for the MMC is less restrictive than the growth of columnar crystals, and the strongest fibers can be chosen for reinforcement. However, unlike the elastic or linear viscoelastic behavior of a composite, the nonlinear, time-dependent response of a metal-matrix composite is not a very well understood subject, and yet its safe application undoubtedly demands a sound theoretical principle which could predict the development of its anisotropic creep strains.

Indeed even for the time-independent (rate-independent) plasticity, theoretical studies—aside from the finite-element calculations—on the overall response of a nonlinear composite are beginning to take shape only very recently. In this connection Talbot and Willis (1985) and Willis (1991) have extended Hashin and Shtrikman's (1963) variational principle to the nonlinear composite, and Ponte Castaneda (1991, 1992) has developed a variational scheme to calculate the bounds (or estimates) of a nonlinear composite from the bounds (or estimates) of a linear "heterogeneous" comparison material. In a separate development, Weng and his associates (Tandon and Weng, 1988; Qiu and

Weng, 1992) have also developed a theory to estimate the elastoplastic behavior of a composite and porous material. Their idea evolved out of Weng's (1982) earlier work on polycrystal plasticity, in which the secant moduli of the polycrystalline matrix were used to characterize its weakening constraint power (Hill, 1965). Initially introduced in the context of Eshelby's (1957) equivalence principle and Mori–Tanaka's (1973) method (Tandon and Weng, 1988), but subsequently with an energy approach to define the effective stress of the heterogeneously deforming matrix (Qiu and Weng, 1992), this approach also makes use of a linear comparison composite, but at the outset takes the elastic properties of the linear matrix to be equal to the secant moduli of the nonlinear matrix. It turned out that, when the nonlinear matrix is also elastically incompressible, the estimates on the stress–strain curves of an isotropic porous material containing randomly oriented spheroidal voids all lie on or below the curve derived from Ponte Castaneda's bound of the Hashin–Shtrikman (1963) type. Comparisons with available exact solutions and finite-element calculations for porous materials and particle-reinforced composites further point to the quantitative accuracy of this approach (one may refer to Qiu and Weng, 1992, for other implications).

As in the time-independent plasticity, the constraint power of the ductile matrix in the time-dependent creep deformation also continues to decrease. This was uncovered recently by Weng (1993) in his consideration of the auxiliary problem of a single spherical inclusion embedded in an incompressible Maxwell solid. Such an auxiliary problem still can not be solved analytically for the present nonlinear problem, and, therefore, to account for such a weakening effect, we shall also introduce a secant-moduli method to study the development of creep strains of a fiber-reinforced composite. This method will be introduced in conjunction with a linear comparison composite and the energy approach, and the contributions from both transient (primary) creep and steady-state (secondary) creep will be considered simultaneously.

2. THE SECANT MODULI OF THE ELASTIC-CREEPING MATRIX

Within the dislocation creep regime where structural metals normally operate, the power-law constitutive equations are suitable for the creep rate. In the triaxial stress state, these can be most conveniently expressed in terms of von Mises' effective stress σ_e and effective creep strain ε_e^c, defined as usual by:

$$\sigma_e = (\tfrac{3}{2}\sigma'_{ij}\sigma'_{ij})^{1/2}, \qquad \varepsilon_e^c = (\tfrac{2}{3}\varepsilon_{ij}^c\varepsilon_{ij}^c)^{1/2}, \tag{1}$$

in terms of the deviatoric stress σ'_{ij} and creep strain ε_{ij}^c. Then the effective steady and transient creep rates may be written as:

$$\begin{aligned} \dot{\varepsilon}_{e(s)}^c &= a\sigma_e^n, \\ \dot{\varepsilon}_{e(t)}^c &= b[d \cdot \sigma_e^n - \varepsilon_e^c], \end{aligned} \tag{2}$$

where a, n, b and d are material constants, derivable from two creep curves at different stress levels. Constant n is the exponent of the power-law constitutive equation; it characterizes the separation of creep curves at different stress levels. Constant a represents the magnitude for the steady creep rate, d controls the magnitude of the transient creep strain, and b signifies the decreasing rate of the transient creep rate. The creep strain ε_e^c in the second equation reflects the influence of strain hardening, and when it reaches the critical value $d \cdot \sigma_e^n$, the transient creep-rate is taken to be zero. As stress exponent n typically lies between 3 and 7 for most metals, the time-dependent creep behavior is said to be nonlinear. The effective creep rate is the sum of the two, $\dot{\varepsilon}_e^c = \dot{\varepsilon}_{e(s)}^c + \dot{\varepsilon}_{e(t)}^c$.

In the two-phase composite we shall refer to the elastic fibers as phase 1 and the ductile, creeping matrix as phase 0. The elastic bulk and shear moduli of the rth phase will be denoted by κ_r and μ_r, respectively, and its volume fraction by c_r. When such a system is subjected to a boundary traction giving rise to a constant stress $\bar{\sigma}_{ij}$ (an overbar signifies the averaged value), the initial response is elastic, with an average stress $\bar{\sigma}_{ij}^{(r)}$ in the rth phase. The subsequent creep deformation in the ductile matrix would lead to a continuous stress transfer from the creeping matrix to the elastic fibers, and, therefore, its effective

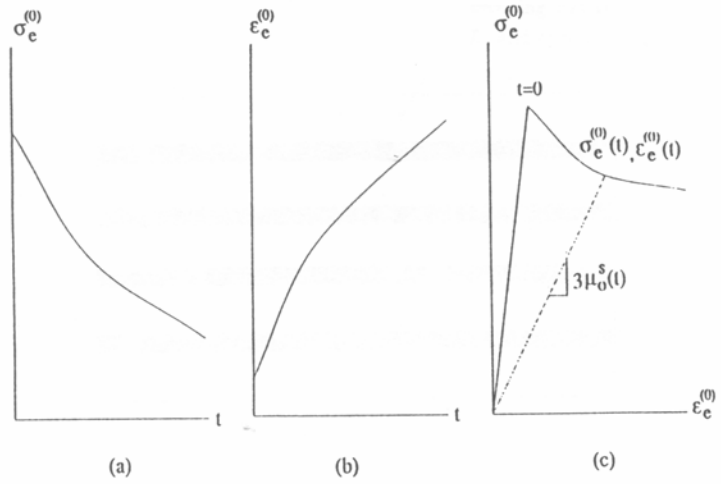

Fig. 1. Schematic diagrams of (a) decreasing effective stress, (b) increasing effective strain and (c) effective stress–strain relation, of the ductile matrix during the time-dependent creep deformation.

stress $\sigma_e^{(0)}$ will continue to decrease. A schematic diagram for such a change is depicted in Fig. 1(a). In the meantime its creep strain will continue to develop. Since the total strain is the sum of the elastic and creep components, the total effective strain of the ductile matrix, $\varepsilon_e^{(0)}$, as depicted in Fig. 1(b), will also continue to grow. Then, using time t as the common factor, the effective stress and total effective strain of the ductile matrix are connected to each other as shown in Fig. 1(c). At time $t = 0$, it represents the initial elastic state, whereas $\sigma_e^{(0)}(t)$ and $\varepsilon_e^{(0)}(t)$ represent a subsequent generic state. The secant shear modulus, $\mu_0^s(t)$, of the elastic-creeping matrix at time t is introduced through:

$$\sigma_e^{(0)}(t) = 3\mu_0^s(t)\varepsilon_e^{(0)}(t), \tag{3}$$

which reduces to the elastic equation initially $\sigma_e^{(0)}(0) = 3\mu_0\varepsilon_e^{(0)}(0)$. Since creep deformation of the ductile matrix is incompressible, its secant bulk modulus remains identical to its elastic counterpart. Then, using Hill's (1965) short-hand notation, the secant moduli tensor L_0^s of the ductile matrix and the elastic moduli tensor L_1 of the fibers can be cast into:

$$L_0^s(t) = (3\kappa_0, 2\mu_0^s(t)), \qquad L_1 = (3\kappa_1, 2\mu_1). \tag{4}$$

The secant Young's modulus, secant Poisson's ratio, and the plane-strain secant bulk modulus of the ductile matrix, respectively, follow as:

$$E_0^s = \frac{9\kappa_0\mu_0^s}{3\kappa_0 + \mu_0^s}, \qquad \nu_0^s = \frac{3\kappa_0 - 2\mu_0^s}{2(3\kappa_0 + \mu_0^s)}, \qquad k_0^s = \kappa_0 + \tfrac{1}{3}\mu_0^s. \tag{5}$$

3. THE LINEAR COMPARISON COMPOSITE

The metal-matrix composite is taken to consist of homogeneously dispersed cylindrical fibers of circular cross-section in the ductile matrix, as schematically shown in Fig. 2(a). Here L_1 and L_0 are taken as the elastic moduli tensors of the fibers and the matrix, respectively, and $\dot{\varepsilon}_e^c = f(\sigma_e, \varepsilon_e^c)$ represents the constitutive eqn (2) of the metal matrix. This composite is subjected to a boundary traction giving rise to a uniform stress $\bar{\sigma}_{ij}$, and, at time t, the secant shear modulus of the creeping matrix is denoted by μ_0^s as defined in (3).

At this instant we introduce a linear comparison composite, as shown in Fig. 2(b), whose microgeometry is identical to the real one and whose fibers also possess the same elastic properties. The bulk and shear moduli of the linear matrix are assigned to be κ_0 and μ_0^s (since the value of μ_0^s decreases continuously it must be updated for the next instant). This comparison composite is also subjected to the same boundary traction as the real one, and the average stress and strain state of the constituents in the real composite are then approximated by those in the linear comparison composite.

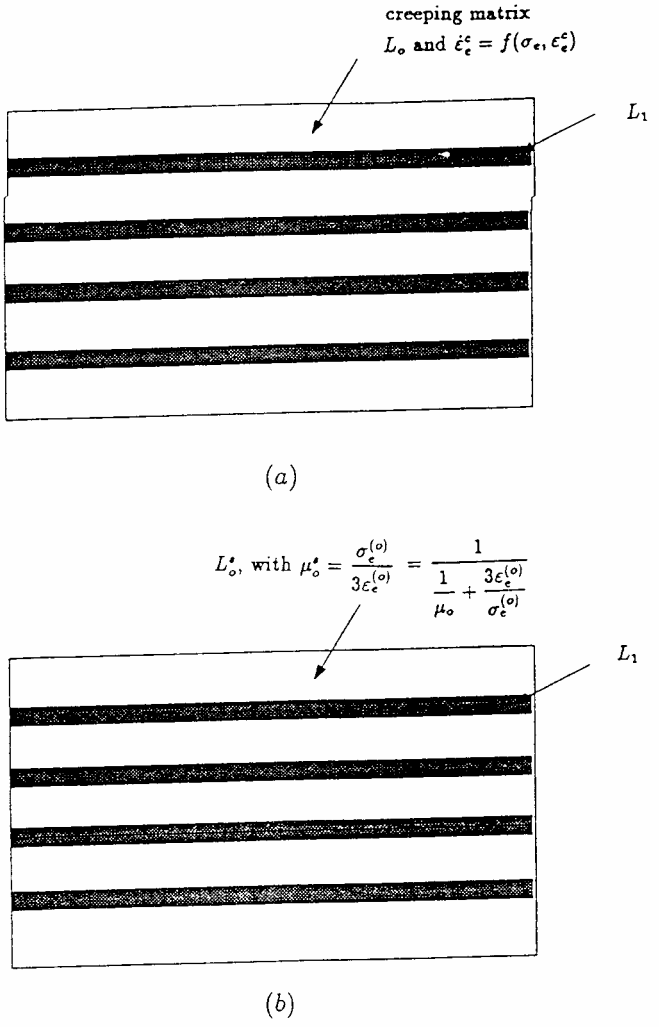

Fig. 2. Schematic diagrams of (a) the real nonlinear, creeping composite and (b) the linear comparison composite.

The many linear theories for the effective elastic moduli of a fiber-reinforced composite can now be called for. In particular, the longitudinal Young's modulus E_{11}^s, major Poisson's ratio ν_{12}^s, plane-strain bulk modulus κ_{23}^s, axial shear modulus μ_{12}^s, and transverse shear modulus μ_{23}^s of the transversely isotropic composite can be written as:

$$
\begin{aligned}
E_{11}^s &= c_1 E_1 + c_0 E_0^s + \frac{4c_1 c_0 (\nu_1 - \nu_0^s)^2}{c_1/k_0^s + c_0/k_1 + 1/\mu_0^s}, \\
\nu_{12}^s &= c_1 \nu_1 + c_0 \nu_0^s + \frac{c_1 c_0 (\nu_1 - \nu_0^s)(1/k_0^s - 1/k_1)}{c_1/k_0^s + c_0/k_1 + 1/\mu_0^s}, \\
\kappa_{23}^s &= k_0^s + \frac{c_1}{1/(k_1 - k_0^s) + c_0/(k_0^s + \mu_0^s)}, \\
\mu_{12}^s &= \mu_0^s + \frac{c_1 \mu_0^s}{\mu_0^s/(\mu_1 - \mu_0^s) + c_0/2}, \\
\mu_{23}^s &= \mu_0^s + \frac{c_1 \mu_0^s}{\mu_0^s/(\mu_1 - \mu_0^s) + (c_0/2)((k_0^s + 2\mu_0^s)/(k_0^s + \mu_0^s))}, \\
E_{22}^s &= \frac{4\kappa_{23}^s}{\kappa_{23}^s/\mu_{23}^s + 1 + 4\nu_{12}^{s2}\kappa_{23}^s/E_{11}^s},
\end{aligned}
\tag{6}
$$

where E_{22}^s is the corresponding transverse Young's modulus, and k_1 the plane-strain bulk modulus of the fibers.

This set of moduli are the familiar Hill's (1964) and Hashin's (1965) lower bounds if the matrix is the softer phase, and are also the results derived from Mori and Tanaka's (1973) mean-field theory. The first four also coincide with those derived by Hashin and Rosen's (1964) composite cylinder model. Christensen and Lo's (1979) μ_{23} may be used for the transverse shear modulus if needed, but the mean stress of the fibers and the matrix—to be used later—must also correspond to those of their generalized self-consistent scheme.

The superscript s added to each of these moduli is meant to underscore their dependence on the time-dependent *secant* moduli of the ductile matrix. It is then apparent that, once the secant shear modulus μ_0^s is determined at time t, the overall strain tensor of the composite follows immediately as:

$$\bar{\varepsilon}(t) = L_s^{-1}(t)\bar{\sigma}, \tag{7}$$

where L_s^{-1} is the inverse of the effective moduli tensor L_s, whose five independent components are given in (6).

4. DETERMINATION OF μ_0^s AND THE ENERGY APPROACH

The determination of $\mu_0^s(t)$ requires the knowledge of $\sigma_e^{(0)}(t)$ and $\varepsilon_e^{(0)}(t)$, as depicted in Fig. 1(c). The elastic component $\varepsilon_e^{e(0)}$ of the effective strain is directly dependent upon $\sigma_e^{(0)}(t)$ through $e_e^{e(0)}(t) = (1/3\mu_0)\sigma_e^{(0)}(t)$, and, once $\sigma_e^{(0)}(t)$ is given for every instant, the constitutive eqns (3) would give the creep rate $\dot{\varepsilon}_e^c(t)$, giving rise to the current knowledge of $\varepsilon_e^c(t)$ in an incremental fashion. Thus the determination of $\mu_0^s(t)$ boils down to the determination of $\sigma_e^{(0)}(t)$.

To this end we note that, unlike in an homogeneous material, the deformation in the ductile matrix of a two-phase composite is generally nonuniform. As depicted in Fig. (3), such a nonuniform field is associated with a uniform mean stress $\bar{\sigma}_{ij}^{(0)}$, but is also accompanied by a locally perturbed stress $\sigma_{ij}^{pt(0)}(x)$, whose volume average over the matrix phase vanishes. In the context of the mean-field approach the effective stress $\sigma_e^{(0)}(t)$ has traditionally been defined in terms of $\bar{\sigma}_{ij}^{(0)}$ alone, following von Mises' definition as given by the first part of eqn (1). While such a definition can capture the essence of deformation under many practical circumstances, it turns out that, if a two-phase isotropic composite is subjected to a purely hydrostatic loading the mean deviatoric components $\bar{\sigma}_{ij}'^{(0)}$ would be zero and the two-phase system would never exhibit the nonlinear response. To overcome such a drawback, Qiu and Weng (1992) recently introduced a new definition for the effective stress $\sigma_e^{(0)}$ of a heterogeneously deformed body based on the concept of distortional energy. Specifically, $\sigma_e^{(0)}$ is defined from the distortional energy density, so that the distortional energy of matrix is given by:

$$U_{0(\text{distortional})}^s = \frac{c_0}{6\mu_0^s}\sigma_e^{(0)2}, \tag{8}$$

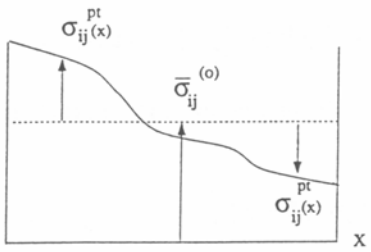

Fig. 3. Schematic diagram of the nonuniform stress field in the ductile matrix.

where

$$U^s_{0(\text{distortional})} = \frac{1}{2}\int_{V_0} \frac{1}{2\mu_0^s}\sigma_{ij}'^{(0)}(x)\sigma_{ij}'^{(0)}(x)\,dV,$$
$$= \frac{1}{4\mu_0^s}[\bar{\sigma}_{ij}'^{(0)}\bar{\sigma}_{ij}'^{(0)} + \langle\sigma_{ij}'^{pt(0)}(x)\sigma_{ij}'^{pt(0)}(x)\rangle], \tag{9}$$

including the contributions from the mean field $\bar{\sigma}_{ij}'^{(0)}$ and the locally perturbed field $\sigma_{ij}'^{pt(0)}(x)$. The angle brackets $\langle\cdot\rangle$ here signify the volume average of the said quantity over its own phase. Thus, the effective stress is in turn defined as:

$$\sigma_e^{(0)^2} = \tfrac{3}{2}(\bar{\sigma}_{ij}'^{(0)}\bar{\sigma}_{ij}'^{(0)} + \langle\sigma_{ij}'^{pt(0)}(x)\sigma_{ij}'^{pt(0)}(x)\rangle). \tag{10}$$

This new definition reduces to the classical one—as in eqn (1)—if the deformation field is uniform, and, for the case where the mean deviatoric stress $\bar{\sigma}_{ij}'^{(0)}$ vanishes—as the isotropic composite mentioned above—the locally perturbed stress can also contribute to the yielding process and the deformation behavior of the two-phase system will still be nonlinear, as desired.

Within this energy framework, we now appeal to the elastic energy of the linear comparison composite, and note that, under a given $\bar{\sigma}_{ij}$, it is given by:

$$U_s = \frac{1}{2}\left[\frac{1}{E_{11}^s}\bar{\sigma}_{11}^2 - \frac{2\nu_{12}^s}{E_{11}^s}\bar{\sigma}_{11}(\bar{\sigma}_{22}+\bar{\sigma}_{33}) + \frac{1}{E_{22}^s}(\bar{\sigma}_{22}+\bar{\sigma}_{33})^2\right.$$
$$\left. - \frac{1}{\mu_{23}^s}\bar{\sigma}_{22}\bar{\sigma}_{33} + \frac{1}{\mu_{23}^s}\bar{\sigma}_{23}^2 + \frac{1}{\mu_{12}^s}(\bar{\sigma}_{12}^2+\bar{\sigma}_{13}^2)\right]. \tag{11}$$

On the other hand a direct evaluation of U_s from its constituents also leads to:

$$U_s = \frac{1}{2}\left[\int_{V_0}\sigma_{ij}^{(0)}(x)\varepsilon_{ij}^{(0)}(x)\,dV + \int_{V_1}\sigma_{ij}^{(1)}(x)\varepsilon_{ij}^{(1)}(x)\,dV\right], \tag{12}$$

where the strain energy from the matrix phase is composed of the distortional and hydrostatic components:

$$\frac{1}{2}\int_{V_0}\sigma_{ij}^{(0)}(x)\varepsilon_{ij}^{(0)}(x)\,dV = \frac{c_0}{2}\left[\frac{1}{3\mu_0^s}\sigma_e^{(0)^2} + \frac{1}{9\kappa_0}(\bar{\sigma}_{kk}^{(0)^2} + \langle\sigma_{kk}^{pt(0)^2}(x)\rangle)\right]. \tag{13}$$

The stress field in the cylindrical fibers $\sigma_{ij}^{(1)}(x)$ and the hydrostatic stress $\sigma_{kk}^{(0)}(x)$ in the matrix are known to be uniform in Hashin and Rosen's (1964) composite-cylinder model for the three boundary-value problems which lead to the first four effective moduli in eqn (6). As a matter of fact, only under the transverse shear (and therefore the transverse tensile) loading are these stress fields not uniform. In this light, and when the fiber concentration is not high, we shall assume both $\sigma_{ij}^{(1)}(x)$ and $\sigma_{kk}^{(0)}(x)$ to be uniform [but not the deviatoric $\sigma_{ij}'^{(0)}(x)$], and the contribution of $\langle\sigma_{kk}^{pt(0)^2}(x)\rangle$ to be negligible. Then,

$$\frac{1}{2}\int_{V_1}\sigma_{ij}^{(1)}(x)\varepsilon_{ij}^{(1)}(x)\,dV = \frac{1}{2}\left(\frac{1}{2\mu_1}\bar{\sigma}_{ij}'^{(1)}\bar{\sigma}_{ij}'^{(1)} + \frac{1}{9\kappa_1}\bar{\sigma}_{kk}^{(1)^2}\right), \tag{14}$$

and substitution of (13) and (14) into (12) will provide the effective stress for the ductile matrix:

$$\sigma_e^{(0)^2} = \frac{6\mu_0^s}{c_0}\left[U_s - \frac{c_0}{18\kappa_0}\bar{\sigma}_{kk}^{(0)^2} - \frac{c_1}{2}\left(\frac{1}{2\mu_1}\bar{\sigma}_{ij}'^{(1)}\bar{\sigma}_{ij}'^{(1)} + \frac{1}{9\kappa_1}\bar{\sigma}_{kk}^{(1)^2}\right)\right], \tag{15}$$

where U_s is given by (11).

The mean stress $\bar{\sigma}_{ij}^{(r)}$ of the rth phase now remains to be determined, but this has already been solved by Zhu and Weng (1990). For the matrix phase, it is given by:

$$\begin{aligned}
\bar{\sigma}_{11}'^{(0)} &= \frac{1}{c_0}\bar{\sigma}_{11}' - \frac{c_1}{c_0^2 p}\frac{1}{1-\mu_0^s/\mu_1}\left[\left(\frac{1}{c_0}\frac{1}{1-\kappa_0/\kappa_1} - \frac{2}{3}\frac{1-2\nu_0^s}{1-\nu_0^s}\right)\bar{\sigma}_{11}' - \frac{1}{9}\frac{1-2\nu_0^s}{1-\nu_0^s}\bar{\sigma}_{kk}\right],\\
\bar{\sigma}_{22}'^{(0)} &= \frac{1}{c_0}\bar{\sigma}_{22}' - \frac{c_1}{c_0^2 p}\left\{\frac{1}{1-\mu_0^s/\mu_1}\left[\left(\frac{1}{c_0}\frac{1}{1-\kappa_0/\kappa_1} - \frac{2}{3}\frac{1-2\nu_0^s}{1-\nu_0^s}\right)\frac{\bar{\sigma}_{22}'+\bar{\sigma}_{33}'}{2}\right.\right.\\
&\quad \left.\left. - \frac{1}{18}\frac{1-2\nu_0^s}{1-\nu_0^s}\bar{\sigma}_{kk}\right] + \frac{c_0 p}{1+c_0(1-\mu_0^s/\mu_1)[3/[4(1-\nu_0^s)]-1]}\frac{\bar{\sigma}_{22}'-\bar{\sigma}_{33}'}{2}\right\},\\
\bar{\sigma}_{33}'^{(0)} &= \frac{1}{c_0}\bar{\sigma}_{33}' - \frac{c_1}{c_0^2 p}\left\{\frac{1}{1-\mu_0^s/\mu_1}\left[\left(\frac{1}{c_0}\frac{1}{1-\kappa_0/\kappa_1} - \frac{2}{3}\frac{1-2\nu_0^s}{1-\nu_0^s}\right)\frac{\bar{\sigma}_{22}'+\bar{\sigma}_{33}'}{2}\right.\right.\\
&\quad \left.\left. - \frac{1}{18}\frac{1-2\nu_0^s}{1-\nu_0^s}\bar{\sigma}_{kk}\right] + \frac{c_0 p}{1+c_0(1-\mu_0^s/\mu_1)[3/[4(1-\nu_0^s)]-1]}\frac{\bar{\sigma}_{33}'-\bar{\sigma}_{22}'}{2}\right\},\\
\bar{\sigma}_{kk}^{(0)} &= \frac{1}{c_0}\bar{\sigma}_{kk} - \frac{c_1}{c_0^2 p}\frac{1}{1-\kappa_0/\kappa_1}\left[\frac{1+\nu_0^s}{2(1-\nu_0^s)}\bar{\sigma}_{11}' + h\bar{\sigma}_{kk}\right],
\end{aligned} \tag{16}$$

where

$$\begin{aligned}
p &= (a+b)\left(\frac{1}{2(1-\nu_0^s)} + a + 2b\right) - 2b\left(\frac{\nu_0^s}{2(1-\nu_0^s)} + b\right),\\
h &= \frac{1}{c_0(1-\mu_0^s/\mu_1)} - \frac{5-4\nu_0^s}{6(1-\nu_0^s)},\\
a &= \frac{1}{c_0(1-\mu_0^s/\mu_1)} - 1,\\
b &= \frac{1}{3c_0}\left(\frac{1}{1-\kappa_0/\kappa_1} - \frac{1}{1-\mu_0^s/\mu_1}\right).
\end{aligned} \tag{17}$$

The mean stress of the fibers follows simply from

$$\bar{\sigma}_{ij}^{(1)} = \frac{1}{c_0}(\bar{\sigma}_{ij} - c_0\bar{\sigma}_{ij}^{(0)}). \tag{18}$$

Equation (15) then provides the effective stress $\sigma_e^{(0)}$ for the ductile matrix at a given stage of deformation; it is implicitly dependent upon μ_0^s.

As the constitutive eqn (2) is given in a rate-form, a forward incremental scheme may be adopted in the calculation. Following the application of $\bar{\sigma}_{ij}$ the composite is initially ($t = 0$) elastic, and thus $\mu_0^s = \mu_0$. This value is used in eqn (6) to calculate the effective elastic moduli of the composite, and by eqn (7) the overall strain. The initial effective stress $\sigma_e^{(0)}$ is also calculated from eqn (15), by setting $\mu_0^s = \mu_0$. Then the initial creep rate of the matrix $\dot{\varepsilon}_e^c$ can be determined from the constitutive eqn (2) (by setting $\varepsilon_e^c = 0$). After a time increment, the new effective creep strain of the ductile matrix becomes:

$$\varepsilon_e^c(t + \mathrm{d}t) = \varepsilon_e^c(t) + \dot{\varepsilon}_e^c(t)\cdot \mathrm{d}t, \tag{19}$$

so that the secant shear modulus changes to:

$$\mu_0^s = \frac{\sigma_e^{(0)}}{3\varepsilon_e^{(0)}} = \frac{\sigma^{(0)}}{3(\sigma_e^{(0)}/3\mu_0 + \varepsilon_e^c)} = \frac{1}{1/\mu_0 + 3\varepsilon_e^c/\sigma_e^{(0)}}, \tag{20}$$

for the next time increment. With this new μ_0^s, the overall secant moduli $E_{11}^s, \nu_{12}^s, \ldots$ in eqn (6) can be determined, and these lead to a new overall strain $\bar{\varepsilon}_{ij}$. In the mean time this new μ_0^s and the newly computed $E_{11}^s, \nu_{12}^s, \ldots$ also result in a new effective stress $\sigma_e^{(0)}$ from eqn (15), and the new creep rate $\dot{\varepsilon}_e^c$ of the matrix can be calculated with this new $\sigma_e^{(0)}$ and the updated effective creep strain ε_e^c. This process can be repeated to obtain the entire strain $\bar{\varepsilon}_{ij}$ vs time curve. The overall creep strain of the composite is given by the difference of its total strain and elastic strain.

5. APPLICATION TO A BORSIC/ALUMINIUM COMPOSITE

The anisotropic nature of creep deformation of a fiber-reinforced metal-matrix composite as calculated from the developed theory will now be demonstrated for a Borsic/aluminium system, and the predicted results will be compared to two existing theories: the mean-field theory developed by Zhu and Weng (1990) for the dilute concentration problem and the local-field theory developed by Wang and Weng (1992). Unlike the secant-moduli method developed here, these two theories were established based on the elastic constraint of the ductile matrix, and, therefore, were intended only for small creep strain range. The assumption of elastic constraint will render the overall creep response somewhat stiffer as deformation proceeds into deep creep range. Furthermore, the mean-field approach to a nonlinear problem will also result in a stiffer response as compared to a local-field approach, except for conditions with dilute concentration under which the deformation field in the ductile matrix is indeed quite uniform, or for a fiber composite under an axial loading which would lead to a relatively uniform field.

The transient and steady creep behavior of an 1100 aluminium has been tested by Ericksen (1973) under pure tension $\bar{\sigma}_{11} = 82.68$ MPa, 65.46 MPa and 41.34 MPa, at room temperature, and the experimental data are reproduced as open circles in Fig. 4 (creep properties at a high temperature had been sought for by the authors, but Ericksen's data were found to be the only ones which provide the creep data for both the ductile matrix and the composite material). With the constitutive eqn (2), these data can be well described with the material constants:

$$a = 8 \times 10^{-13}, \qquad n = 4, \qquad b = 8, \qquad d = 7.7 \times 10^{-11}, \tag{21}$$

where stress, strain and time are in the units of MPa, m/m, and h, in turn. The simulated creep curves with these constants are plotted alongside, reflecting a reasonable accuracy.

Borsic fibers can also creep, but Ericksen's data and Wang and Weng's (1992) calculations both indicate that its contribution to the overall creep of the composite is less than 1%, and thus will be neglected. The elastic moduli of both phases are (Ericksen, 1973; Allred *et al.*, 1974):

$$\begin{aligned} &\text{Borsic fibers:} && E_1 = 392.7\ \text{GPa}, && \nu_1 = 0.15; \\ &\text{Aluminium matrix:} && E_0 = 68.9\ \text{GPa}, && \nu_0 = 0.33. \end{aligned} \tag{22}$$

Using these material constants and the theory developed, we then calculated the development of creep strain. To reflect the creep deformation of a compressor or turbine blade under a centrifugal force, we first subject the composite to an axial tension $\bar{\sigma}_{11} = 100$ MPa. To provide a background for comparison, the total creep strain $\bar{\varepsilon}^c_{11}$ of the composite as calculated by Zhu and Weng's (1990) mean-field theory and Wang and

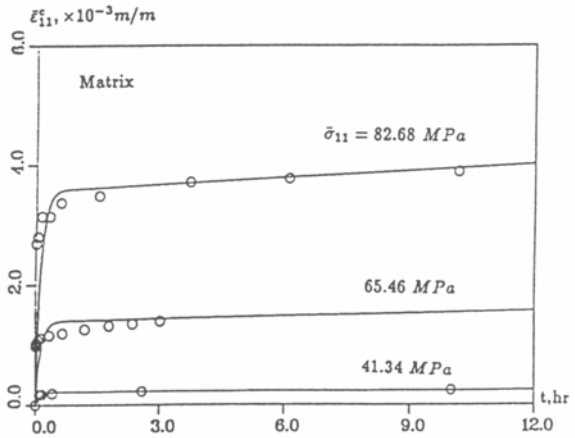

Fig. 4. Creep properties of a 1100 aluminium at room temperature.

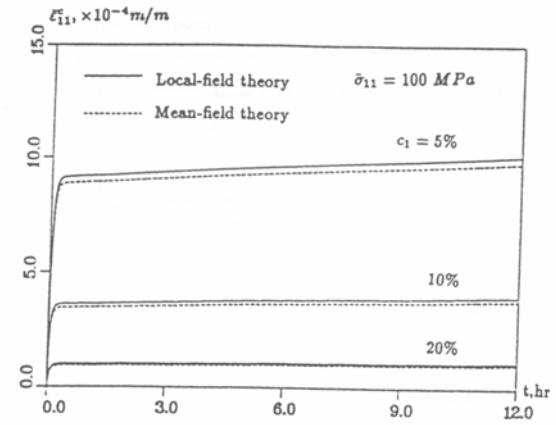

(a)

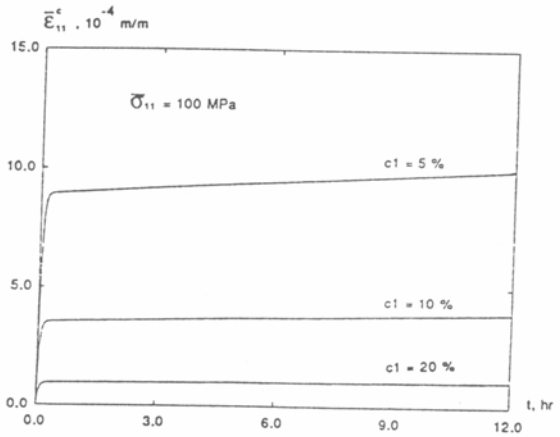

(b)

Fig. 5. Development of the axial tensile creep strains by (a) the elastic constraint approximation, with the mean-field and local-field approaches and (b) the secant-moduli approach.

Weng's (1992) local-field theory are plotted in Fig. 5(a) at three selected fiber concentrations: $c_1 = 5\%$, 10% and 20%. The axial creep strains calculated by the present theory are shown in Fig. 5(b). While the prediction by the mean-field theory is stiffer than the local theory and the secant-moduli method developed here, the somewhat uniform field in the ductile matrix under an axial loading has clearly rendered the mean-field approach a rather accurate one even at the concentration of 20%.

This however is not the case under a transverse loading, say at $\bar{\sigma}_{22} = 100$ MPa. The deformation of the composite is now matrix-dominated, and the field in the matrix is rather nonuniform. The overall transverse creep strains $\bar{\varepsilon}^c_{22}$ are now depicted in Fig. 6(a) and 6(b), again for the same three selected fiber concentrations. The predictions by the mean-field theory are now noticeably stiffer than the local one, which, due to its elastic-constraint assumption, in turn also leads to a stiffer response than the current secant-moduli approach. The calculation by the local theory involves a rather elaborate accounting of the local stress and strain fields of the heterogeneously deforming matrix (Luo and Weng, 1989). When the local information is needed (say for the determination of matrix cracking or void growth) or when the fiber concentration is high, the local approach should be called for. But for estimating the overall response at low or moderate concentration, the present theory is the simpler one.

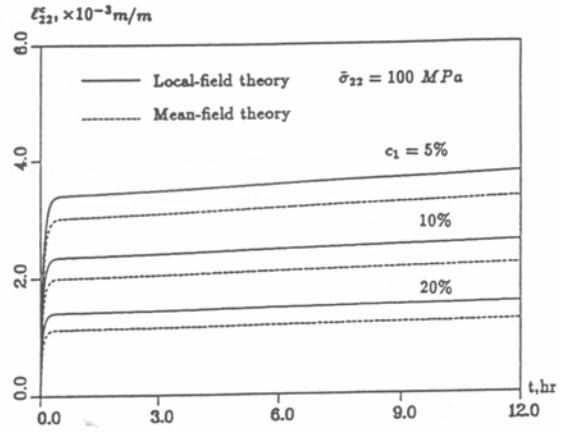

(a)

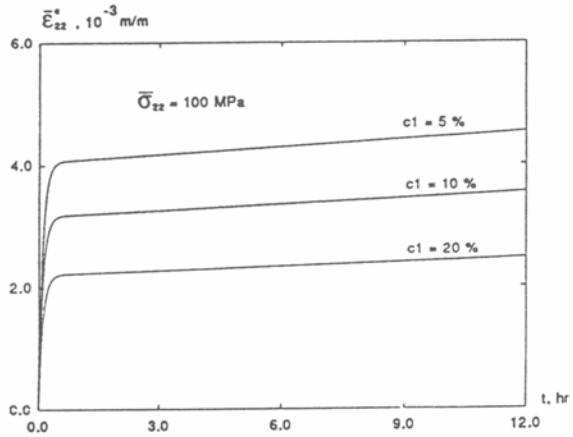

(b)

Fig. 6. Development of the transverse tensile creep strains by (a) the elastic constraint approximation, with the mean-field and local-field approaches and (b) the secant-moduli approach.

The creep behavior under plane-strain, biaxial loading with an initial, macroscopic effective stress $\bar{\sigma}_e(0) = 100$ MPa are given in Fig. 7(a) and 7(b). The plane-strain condition ($\bar{\varepsilon}_{11} = 0$) implies that $\bar{\sigma}_{11} = \nu^s_{12}(\bar{\sigma}_{22} + \bar{\sigma}_{33})$, and in this case the biaxial stresses are $\bar{\sigma}_{22} = \bar{\sigma}_{33} = 100/(1 - 2\nu^s_{12})$, initially with $\nu^s_{12} = \nu_{12}$. As ν^s_{12} is not constant, the biaxial stress must also be adjusted to maintain the plane-strain condition as deformation proceeds. The relative features of these three theories remain similar to those in Fig. 6. The level of creep strain, however, is two orders of magnitude lower than the transverse creep, and one order less than the axial creep.

The accuracy of the theory is now partially assessed by a comparison with the experiment under the transverse tension $\bar{\sigma}_{22} = 65.46$ MPa, at the fiber concentration $c_1 = 35\%$. Both the theoretical prediction and the experimental data for the evolution of total strain (the sum of elastic and creep strains) are shown in Fig. 8. Also included as a background curve on the top is the total strain curve of the pure aluminium matrix under the same stress. The superior creep resistance of the composite is evident (of course it is even more so under axial tension), and the accuracy of the theory is seen to be quite satisfactory.

Finally, we note that, among all possible loading directions, transverse tension is known to be the most critical one in causing the interfacial debonding. The maximum

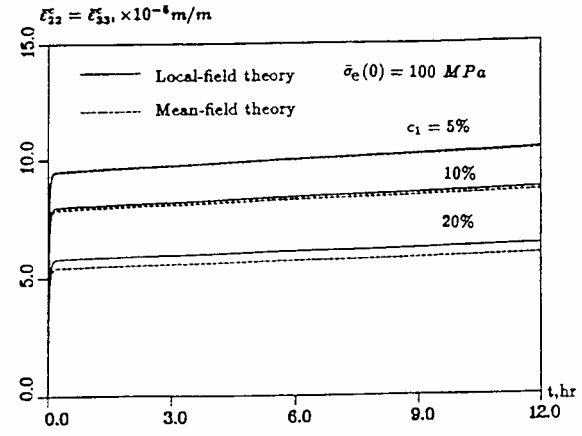

(a)

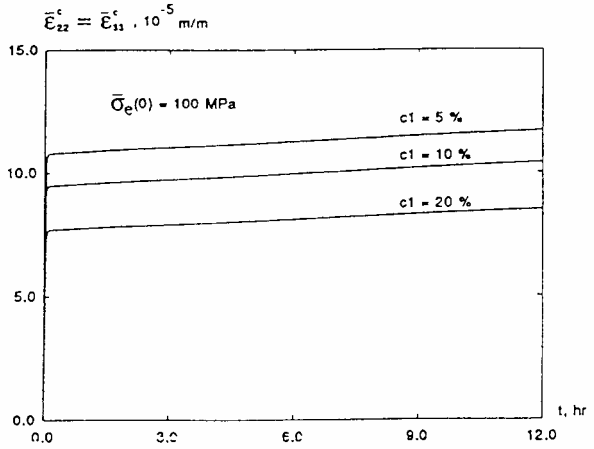

(b)

Fig. 7. Development of the biaxial tensile creep strains by (a) the elastic constraint approximation, with the mean-field and local-field approaches and (b) the secant-moduli approach.

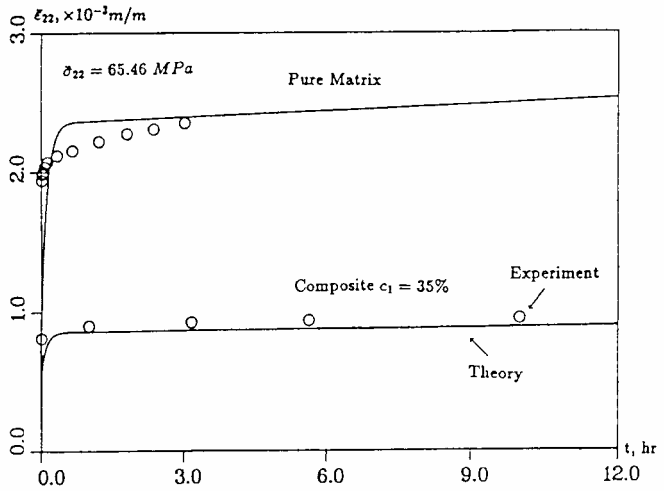

Fig. 8. Comparison between the secant-moduli approach and the experimental data under a transverse tension.

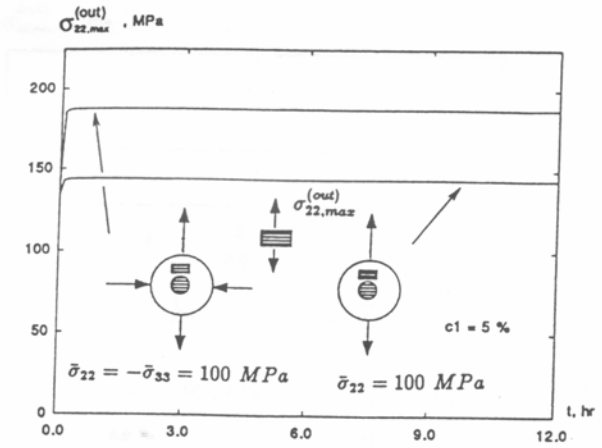

(a)

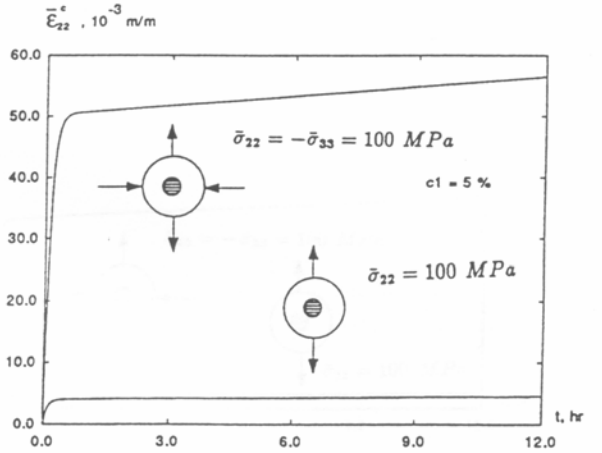

(b)

Fig. 9. Development of (a) the maximum interfacial tensile stress and (b) the transverse tensile creep strain of the composite, under a transverse tension with and without a superimposed lateral compression at $c_1 = 5\%$.

tensile stress in this case occurs at the pole, whose tensile stress evolution under $\bar{\sigma}_{22} = 100$ MPa is depicted as the lower curve in Fig. 9(a), at $c_1 = 5\%$. The stress concentration increases from 1.38 initially to 1.44 after 12 h. When such a transverse loading is superimposed by a lateral compression $\bar{\sigma}_{33} = -\bar{\sigma}_{22} = -100$ MPa, the tensile stress concentration is significantly higher, increasing to 1.88 at $t = 12$ h. The most drastic effect for such a superimposed compression is in the generated tensile creep strain $\bar{\varepsilon}_{22}^{c}$ for the composite; as shown in Fig. 9(b), it is about 12 times higher at the end of 12 h. Such a dramatic effect is due to the nonlinear stress exponent $n = 4$, in the constitutive equation.

To reflect the influence of fiber concentration on the evolution of the maximum tensile interfacial stress and the overall transverse strain with and without a superimposed lateral compression, similar results are plotted in Fig. 10(a) and (b), at $c_1 = 20\%$. The increase of fiber volume fraction has resulted in a lower stress concentration, but as shown by the top curves of Fig. 10(a) and (b), a superimposed lateral compression has also led to significant increase in both the stress concentration and the accumulation of the overall transverse creep strain.

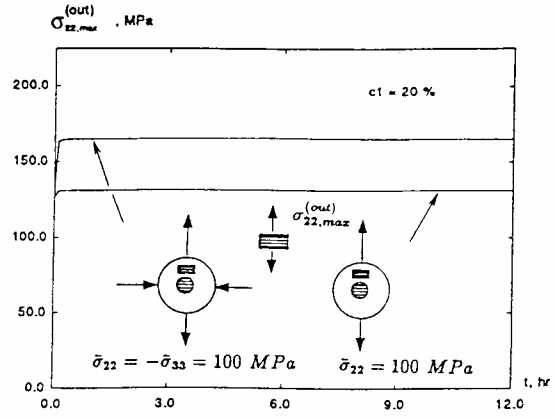

(a)

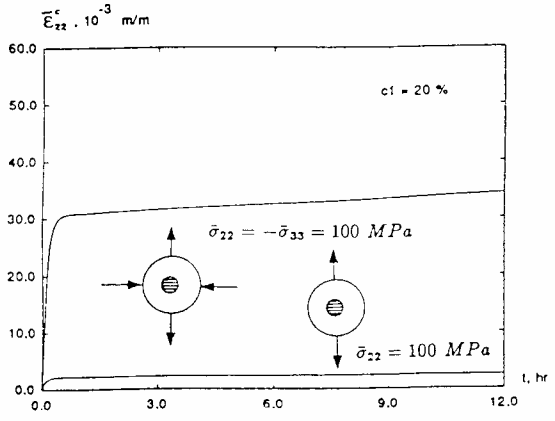

(b)

Fig. 10. Development of (a) the maximum interfacial tensile stress and (b) the transverse tensile creep strain of the composite, under a transverse tension with and without a superimposed lateral compression at $c_1 = 20\%$.

Acknowledgement—This work was supported by the National Science Foundation, Mechanics and Materials Program, under Grant MSS-9114745.

REFERENCES

Allred, R. E., Hoover, W. R. and Horak, J. A. (1974). Elastic-plastic Poisson's ratio of borsic-aluminium. *J. Composite Mater.* **8**, 15–28.

Christensen, R. M. and Lo, K. H. (1979). Solutions for effective shear properties in three phase sphere and cylinder models. *J. Mech. Phys. Solids* **27**, 315–330.

Ericksen, R. H. (1973). Room temperature creep of Borsic-aluminum composites. *Metall. Trans.* **4A**, 1687–1693.

Eshelby, J. D. (1957). The determination of elastic field of an ellipsoidal inclusion, and related problems. *Proc. R. Soc. Lond.* **A241**, 376–396.

Hashin, Z. (1965). On elastic behaviour of fiber-reinforced materials of arbitrary transverse phase geometry. *J. Mech. Phys. Solids* **13**, 119–134.

Hashin, Z. and Rosen, B. W. (1964). The elastic moduli of fiber-reinforced materials. *J. appl. Mech.* **31**, 223–232.

Hashin, Z. and Shtrikman, S. (1963). A variational approach to the theory of the elastic behavior of multiphase materials. *J. Mech. Phys. Solids* **11**, 127–140.

Hill, R. (1964). Theory of mechanical properties of fiber-strengthened materials: I. Elastic behaviour. *J. Mech. Phys. Solids* **12**, 119–212.

Luo, H. A. and Weng, G. J. (1989). On Eshelby's S-tensor in a three phase cylindrically concentric solid, and the elastic moduli of fiber-reinforced composites. *Mech. Mater.* **8**, 77–88.

Mori, T. and Tanaka, K. (1973). Average stress in the matrix and average elastic energy of materials with misfitting inclusions. *Acta Metall.* **21**, 571–574.

Ponte Castaneda, P. (1991). The effective mechanical properties of nonlinear isotropic composites. *J. Mech. Phys. Solids* **39**, 45–71.

Ponte Castaneda, P. (1992). New variational principles in plasticity and their application to composite materials. *J. Mech. Phys. Solids* **40**, 1757–1788.

Qui, Y. P. and Weng, G. J. (1992). A theory of plasticity for porous materials and particle-reinforced composites. *J. appl. Mech.* **59**, 261–268.

Talbot, D. R. S. and Willis, J. R. (1985). Variational principles for inhomogeneous nonlinear media. *IMA J. appl. Math.* **35**, 39–54.

Tandon, G. P. and Weng, G. J. (1988). A theory of particle-reinforced plasticity. *J. appl. Mech.* **55**, 126–135.

Wang, Y. M. and Weng, G. J. (1992). Transient creep strain of a fiber-reinforced metal–matrix composite under transverse loading. *ASME J. Engng Mater. Technol.* **114**, 237–244.

Weng, G. J. (1982). A unified self-consistent theory for the plastic-creep deformation of metals. *J. appl. Mech.* **49**, 728–734.

Weng, G. J. (1993). A self-consistent relation for the time-dependent creep of polycrystals. *Int. J. Plasticity* **9**. 181–198.

Willis, J. R. (1991). On methods for bounding the overall properties of nonlinear composites. *J. Mech. Phys. Solids* **39**, 73–86.

Zhu, Z. G. and Weng, G. J. (1990). Creep anisotropy of a metal–matrix composite containing dilute concentration of aligned spheroidal inclusions. *Mech. Mater.* **9**, 93–105.